

# HOW TO LIMIT THE HEAT LOSS OF ANODE STUBS AND CATHODE COLLECTOR BARS IN ORDER TO REDUCE CELL ENERGY CONSUMPTION

Marc Dupuis  
GéniSim Inc., 3111 Alger St., Jonquière, Québec, Canada G7S 2M9  
marc.dupuis@genisim.com

Keywords: Mathematical modeling; power efficiency; copper collector bars; cell heat balance

## Abstract

At last year TMS, the author presented the design of cells operating at around 11 kWh/kg Al. Those designs rely on the usage of design features to limit the heat loss of anode stubs and cathode collector bars that were not revealed in last year paper. Those design features are now revealed and explained.

Furthermore, the mathematical models used to analyze design options have been modified to better calculate the impact of those design features on the cell heat balance and explore with more accuracy design options to further reduce the cell power consumption while maintaining a manageable cell superheat.

## Introduction

Designing a very low energy consumption cell could be considered more challenging than designing a very high amperage cell. In order to reduce the cell energy consumption, first the cell operating voltage must be reduced. This is done by reducing the ohmic components of the cell voltage, namely the anode, the cathode and the bath voltage drops.

For the anode and the cathode voltage drops, this is done by selecting the proper materials and design as presented in the author TMS 2017 paper [1]. For the bath voltage drop, this is done by using slotted anodes to minimize the bubble resistance [2] and by operating at the minimum ACD possible.

Contrary to conventional wisdom, operation below 4 cm at high current efficiency is possible. Operation at 2.8 cm of ACD and 95% of current efficiency has been reported by EGA in [3]. Of course, the absolute value of the ACD has only meaning if we know how it was calculated. For that purpose, one very popular reference is Haupin [4]. The equations presented in [4] have been coded in the HHCellVolt code available on Peter Entner website [5] for everyone to use and hence report comparable ACD values.

Operating at very low cell voltage in order to minimize the cell energy consumption means operating at an extremely low cell internal heat generation. The cell internal heat is the excess of electrical energy not use to produce the metal. Hence in order to calculate the cell internal heat, the energy required to produce the metal must be calculated first. In recent years, work has been done to produce more precise enthalpy calculations involving more than the main aluminum electrolysis reaction. Per example [3] also reports the calculation of the impact of auxiliary processes like the heating of the cover material on the energy requirement to produce the metal in Table 2.

In the case presented, an extra energy requirement of about 0.25 kWh/kg in addition to the minimum 6.34 kWh/kg requirement to carry out the basic reaction has been reported. This leads Barry Welch in [6] to recommend to use 6.6 kWh/kg in place of 6.34 kWh/kg as estimate for the required energy to produce the metal.

HHCellVolt incorporates all the enthalpy calculations required to compute with accuracy the energy to make the metal assuming that one knows with precision all the auxiliary processes taking place in the cells [7].

In any case, for operation at very low cell voltage, the excess of electrical energy not used to produce the metal i.e. cell internal heat becomes extremely low as reported in [1] and more recently in [8, 9]. This fact constitutes the second challenge in designing a very low energy consumption cell, as the cell still needs to operate at a manageable cell superheat and ledge thickness.

In that context, the accuracy of the calculation of cell internal heat is critical hence the recent effort to improve the evaluation of the energy required to produce the metal. It is also critically important to measure and model accurately the cell heat balance. In that context, the author felt the need to improve the way its models calculate the cell heat balance.

## Improvement of the model calculated cell heat balance

The heat balance calculation of any system is based on the establishment of the boundary of that system. For the calculation of a cell heat balance several boundaries can be used. Figure 1 of [3] reproduced here in Figure 1 presents two of those possible boundaries.

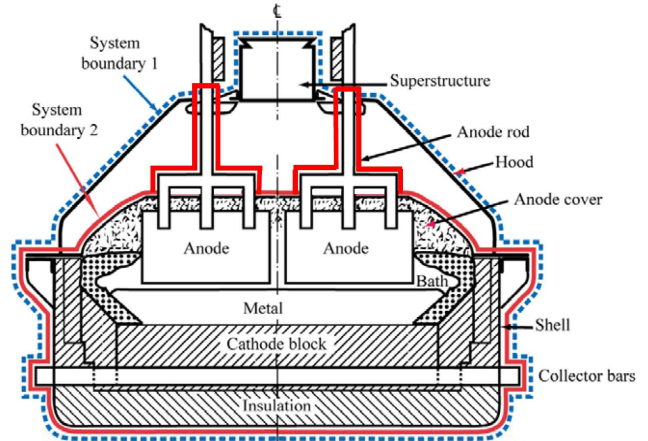


Figure 1: Two of the possible cell boundaries that can be used to calculate the cell heat balance (Figure 1 in [3])

The solid red line boundary in Figure 1 is very convenient as it exactly incorporates the domain of the full anode and cathode. For that reason, it is the boundary used by the author's mathematical models to calculate the cell heat balance since their conception in the 80's [10].

Yet, the cell boundary that really matters, as far as the cell internal conditions are concerned, is the boundary presented in Figure 10 of [11], one of the best classical reference on the subject of cell heat balance.

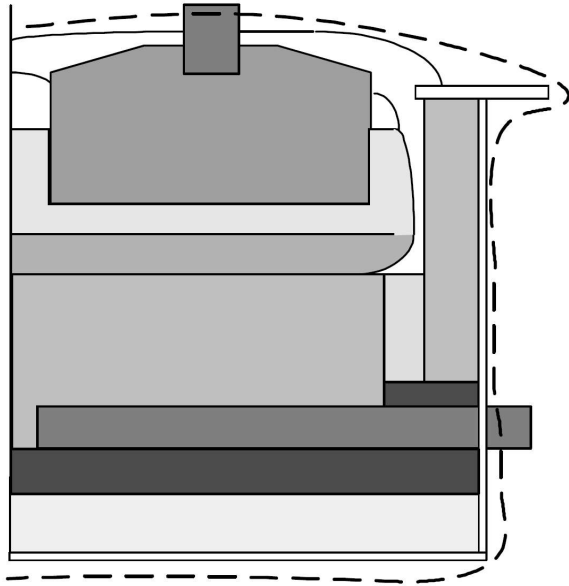


Figure 2: The best possible cell boundary that can be used to calculate the cell heat balance (Figure 10 in [11])

That boundary cuts through the anode stubs and cathode collector bars to establish the cell internal domain. It is the heat dissipated by conduction out of the cell by the stubs and collector bars that matters to define the cell internal conditions. The reason being that the external electrical network that conducts the current from one cell to the next truly starts where the collector bars exit from the cell and end where the anode stubs of the next cell are buried by the anode cover material.

This boundary is less practical to use to measure the cell heat balance, as it requires measuring the thermal gradient in the stubs and bars. It is also less practical to report the model results as it does not match the model boundary. Since to design very low energy consumption cells, we need to concentrate on reducing the heat dissipated by the stubs and collector bars, it is becoming critical for accuracy purpose to use that best possible boundary to analyze the cell heat balance.

#### Revealing the design feature that reduces the stubs and collector bars heat loss

Since the introduction of a massive copper collector bar in its 600 kA "retrofit" design in 2011 [12], the author has been using a design feature that prevents that massive copper bars to dissipate an excessive amount of heat. That design feature is a quite significant reduction of the copper collector bar section just before going out of the potshell.

So far in [12] and other publications, the cathode model has been displayed in a way that avoids showing the geometry of the bar going out. Figure 3 displays the mesh of the 600 kA cathode model showing that 2/3 of the collector bar section has been removed.

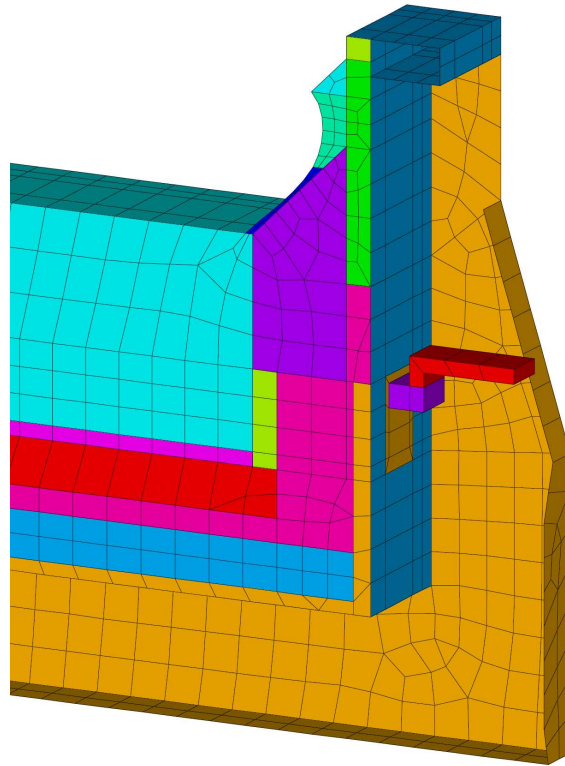


Figure 3: 600 kA cathode side slice model initial mesh

Figure 4 shows the corresponding cathode voltage drop solution, displaying that the copper collector bar section has been reduced in the pier region.

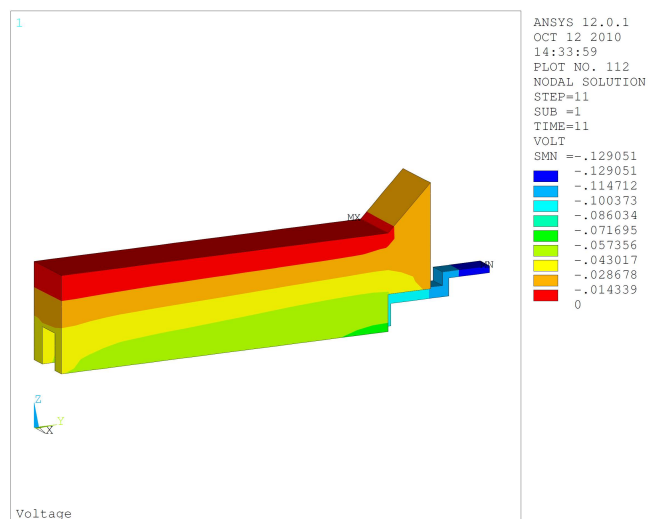


Figure 4: 600 kA cathode side slice model voltage solution

The temperature solution with the converged ledge profile is presented in Figure 7 of [12] and again here in Figure 5. That model predicted ledge thickness is very much affected by that specific choice of copper collector bar geometry. The solution would be very different if the copper bar section would have remained the same all the way up to the end of the bar.

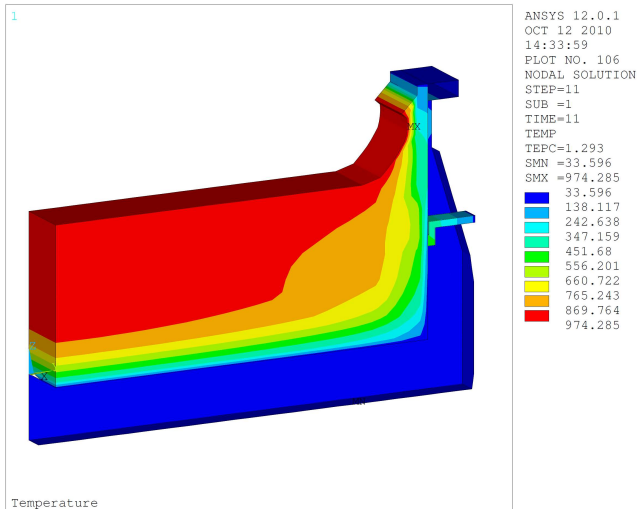


Figure 5: 600 kA cathode side slice model temperature solution

In 2011, the aim was not to significantly reduce the collector bars heat loss but rather to prevent the massive copper collector bars used in that design to dissipate an increased amount of heat. In the 500 kA, 11.2 kWh/kg cell design presented in [8], the section of the copper collector bar going out of the cell was further reduced, this time to significantly decrease the collector bars heat loss.

The same design feature can also be used to limit the anode stubs heat loss. Per example, the anode design of the 500 kA cell presented in [8] uses that design feature. Figure 6 presents the geometry of the 500 kA half anode model without the cover material revealing that temporary stub diameter reduction design feature used to decrease the stubs heat loss.

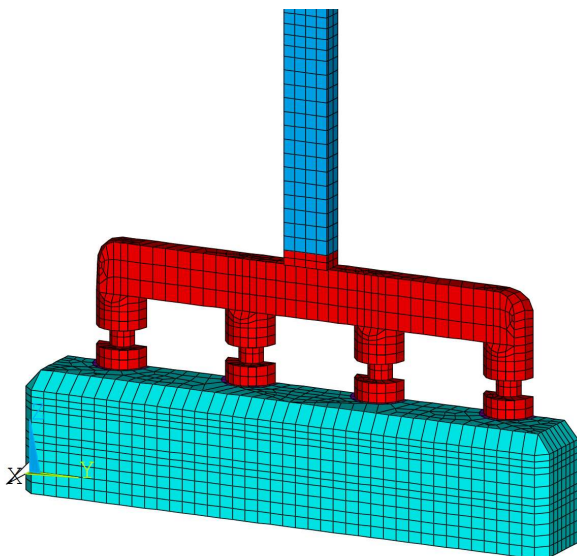


Figure 6: 500 kA half anode model mesh without the cover

Figure 7 presents the corresponding voltage solution. There is obviously a small voltage penalty in temporarily reducing the stubs diameter but when designing a very low energy consumption cell, the advantage in reducing the stubs heat loss far exceeds the inconvenient of that small voltage penalty.

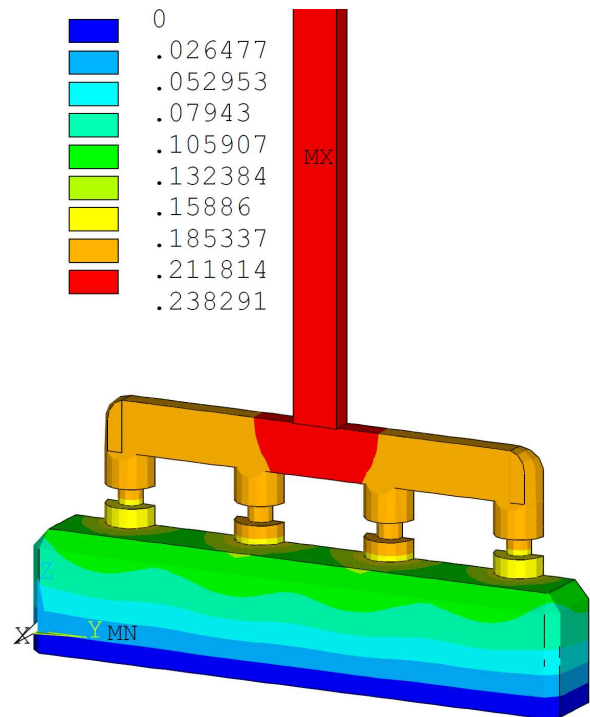


Figure 7: 500 kA half anode model voltage solution

Figure 8 presents the corresponding temperature solution highlighting the effect of the stub diameter restriction on the thermal gradient in the stubs. This type of design allows the use of bigger stub diameter in order to reduce the voltage drop between the cast iron and the carbon without increasing the stubs heat loss. On the contrary, this special stub design feature allows to quite significantly reduce the stubs heat loss regardless of the selected stub diameter.

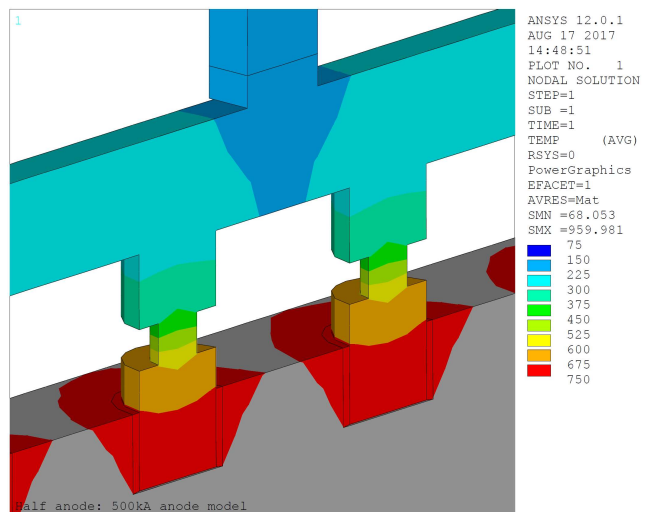


Figure 8: 500 kA half anode model temperature solution

**Partial Review of the Intellectual Property related to this “special” but not “new” design feature**

When the author started to use what he thought was a completely new design feature to reduce the heat loss of his massive copper collector bars, he did not look for the existence of patents that could already exist on the subject. Same thing when he later started to use the same design feature to reduce the heat loss of anode studs.

Yet after having used this “special” design feature in its anode stub design, the author discovered the existence of a Pechiney 1985 patent [13] protecting that exact design feature for anode stubs. Figure 9 is presenting figure 4 of [13]. So, it is not a “new” design feature after all!

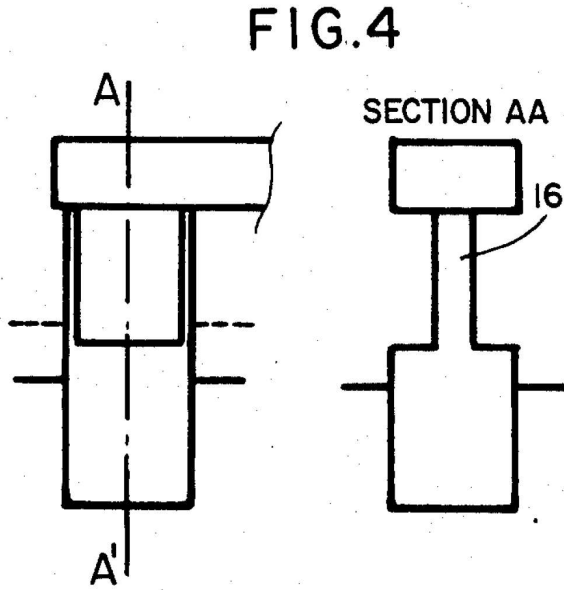


Figure 9: Heat loss reduction design feature protected by the 1985 Pechiney patent [13]

In their TMS paper on the APXe [14], Rio Tinto researchers wrote the following:

- *Anode conductors*: the thermal losses by the anode assembly were reduced by means of a technical innovation which reduces the losses through the stubs and the yoke by 20%, without increasing the anode resistance.

Regarding the state of the art, no other ways to reduce stub heat losses have been reported apart [13]. So, when looking at [14], and regarding the existing state of the art, it is likely that [14] uses technical solution such as [13].

Through a consulting mandate with EGA, the author revealed his design feature to reduce the collector bar and stubs heat loss and the existence of the 1985 Pechiney patent. EGA later responded by filling a patent application [15] that is trying to protect an alternative way to achieve the same stub section temporary restriction by drilling a hole perpendicular to the stub center axis as presented in Figure 10 which is Figure 2 in [15] with an insert of Figure 4 in [15]. This alternative way to restrict the stub heat dissipation meets the principle of [13].

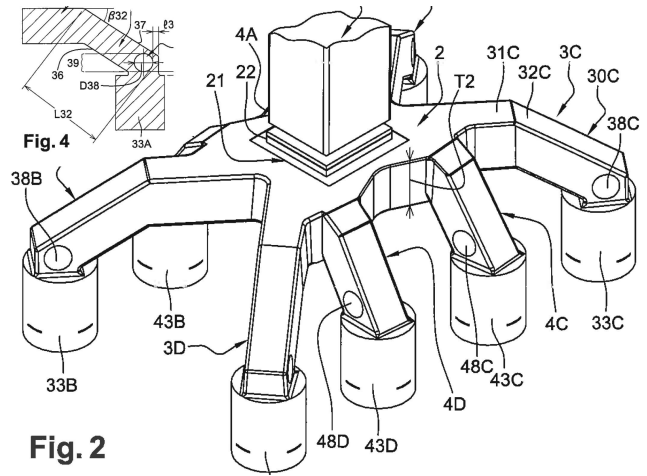


Figure 10: Heat loss reduction design feature protected by the 2017 EGA patent application [15]

**520 kA cell with 100% downstream side current extraction**

The lowest energy consumption cell design presented so far by the author is the 10.85 kWh/kg 520 kA cell with 100% downstream side current extraction published in [9]. The models heat balance results of that cell design have been recalculated using the new heat balance cell boundary previously presented above. Table I is presenting the new model predicted anode heat balance while Table II is presenting the new model predicted cathode heat balance. Table III compares the results of the 520 kA cell calculated using the old and the new cell boundary to calculate the cell heat balance.

Table I: Anode heat balance

**** HEAT BALANCE TABLE ****			
**** Half Anode Model : 520 KA ****			
ANODE PANEL HEAT LOST	kW	W/m <sup>2</sup>	%
Crust to air	86.32	1138.04	30.13
Stubs in to stubs out	200.16		69.87
<b>Total Anode Panel Heat Lost</b>	<b>286.48</b>		<b>100.00</b>

Table II: Cathode heat balance

**** HEAT BALANCE TABLE ****			
**** Side Slice Model : 520 KA ****			
CATHODE HEAT LOST	kW	W/m <sup>2</sup>	%
Shell wall above bath level	47.24	779.79	12.39
Shell wall opposite to bath	35.26	3621.94	9.25
Shell wall opposite to metal	22.68	5126.01	5.95
Shell wall opposite to block	59.58	2358.01	15.62
Shell wall below block	7.67	397.16	2.01
Shell floor	30.46	373.83	7.99
Cradle above bath level	2.05	937.15	0.54
Cradle opposite to bath	9.63	1404.07	2.53
Cradle opposite to metal	3.78	1615.84	0.99
Cradle opposite to block	17.85	386.87	4.68
Cradle opposite to brick	3.34	75.50	0.88
Cradle below floor level	35.63	97.53	9.34
Bar in to bar out	123.99		32.51
Cathode bottom estimate	239.79		62.88
<b>Total Cathode Heat Lost</b>	<b>381.34</b>		<b>100.00</b>

Table III: Design and predicted operational data

Amperage	520 kA	520 kA
Nb. of anodes	64	64
Anode size	1.95 m X .5 m	1.95m X .5m
Nb. of anode stubs	4 per anode	4 per anode
Anode stub diameter	17.5 cm	17.5 cm
Anode cover thickness	20 cm	20 cm
Nb. of cathode blocks	24	24
Cathode block length	4.17 m	4.17 m
Type of cathode block	HC10	HC10
Collector bar size	20 cm X 20 cm	20 cm X 20 cm
Type of side block	HC3	HC3
Side block thickness	7 cm	7 cm
ASD	30 cm	30 cm
Calcium silicate thickness	6.0 cm	6.0 cm
Inside potshell size	17.8 mX4.85 m	17.8 mX4.85 m
ACD	2.8 cm	2.8 cm
Excess AlF <sub>3</sub>	12.00%	12.00%
Anode drop (A)	248 mV	210 mV
Cathode drop (A)	128 mV	124 mV
Busbar drop (A)	85 mV	127 mV
Anode panel heat loss (A)	295 kW	286 kW
Cathode total heat loss (A)	404 kW	381 kW
Operating temperature (D/M)	958.3 °C	957.7 °C
Liquidus superheat (D/M)	5.3 °C	4.7 °C
Bath ledge thickness (D/M)	20.0 cm	22.8 cm
Metal ledge thickness (D/M)	15.3 cm	18.1 cm
Current efficiency (D/M)	96.5%	96.5%
Internal heat (D/M)	701 kW	679 kW
Energy consumption	10.85 kWh/kg	10.85 kWh/kg

As we can see in Table III, the cell energy consumption prediction is not affected as the cell voltage and current efficiency remained the same but the cell internal heat and cell superheat prediction has been affected by the change of cell boundary definition.

#### 475 kA cell with 100% downstream side current extraction

Equipped with this improved modeling tool, a new round of cell retrofit design has been performed with the aim to further reduce the cell energy consumption. On the cell voltage side, considering that the minimum possible ACD reported in literature is about 2.8 cm, the only possible way to further significantly reduce the cell voltage is by reducing the anode current density hence reducing the cell amperage. At 520 kA, the anode current density is 0.83 A/cm<sup>2</sup>. By reducing the cell amperage to 475 kA, the anode current density drops to 0.76 A/cm<sup>2</sup>. That was approximately the usual anode current back in the 70's when the AP18 was designed per example. To further reduce the external voltage drop, the busbar section was further increase despite the reduction of the line amperage. Figure 11 presents the new busbar voltage solution obtained.

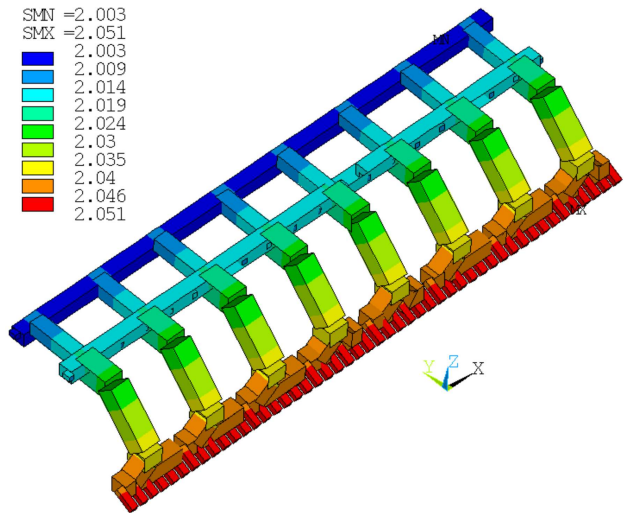


Figure 11: 475 kA busbar voltage solution

The anode stub diameter was increased to 20 cm and the yoke and rod sections were also increased in order to further decrease the anode voltage drop. In order to further decrease the anode heat loss, the decreased stub section was further reduced as shown in Figure 12. Table IV presents the new anode heat balance.

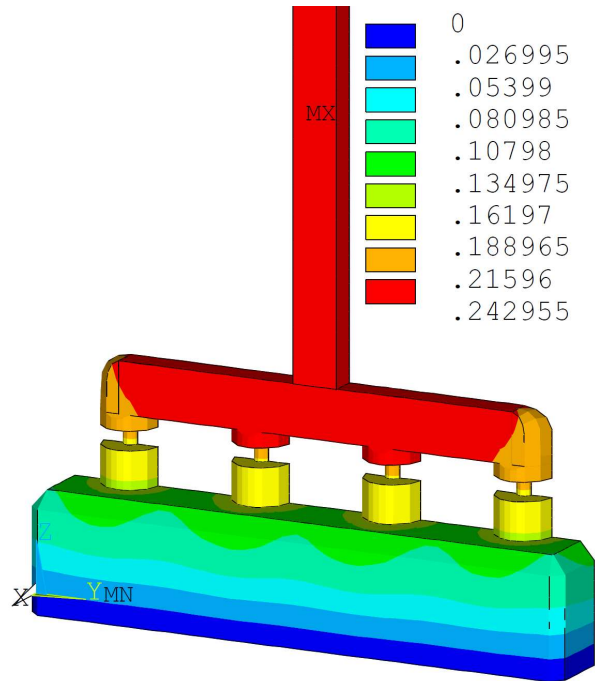


Figure 12: 475 kA half anode model voltage solution

Table IV: Anode heat balance

**** HEAT BALANCE TABLE ****			
**** Half Anode Model : 475 kA ****			
ANODE PANEL HEAT LOST	kW	W/m <sup>2</sup>	%
Crust to air	121.69	1495.75	51.08
Stubs in to stubs out	116.56		48.92
Total Anode Panel Heat Lost	238.25		100.00

As Table IV is showing, despite the drastic reduction of the decreased stub section, the stub heat loss still represents about half of the anode heat loss. Despite the increase of the stub diameter and the decrease of the cell amperage, the internal portion of the anode voltage drop remained essentially unchanged at 208 mV due to this drastic reduction of the decreased stub section.

On the cathode side, the only change is a drastic reduction of the decreased collector bar section, which significantly reduced the collector bars heat loss but unfortunately also significantly increases the cathode voltage drop despite the reduction of cell amperage. The decreased collector bar section is shown in Figure 13. Table V presents the new cathode heat balance.

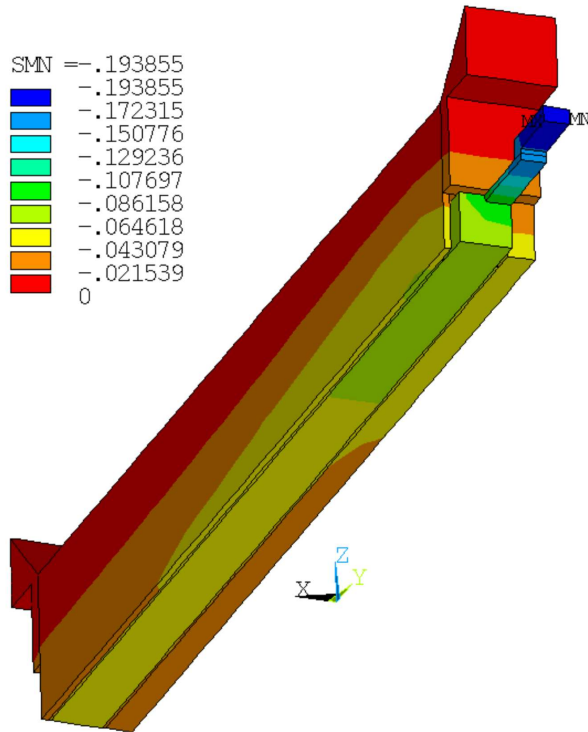


Figure 13: 475 kA cathode model voltage solution

Table V: Cathode heat balance

```

****      HEAT BALANCE TABLE      ****
****      Side Slice Model : 475 kA      ****

```

CATHODE HEAT LOST	kW	W/m <sup>2</sup>	%
Shell wall above bath level	45.39	781.41	13.67
Shell wall opposite to bath	33.93	3634.74	10.22
Shell wall opposite to metal	21.85	5150.46	6.58
Shell wall opposite to block	57.58	2376.71	17.34
Shell wall below block	7.72	417.04	2.32
Shell floor	31.20	382.96	9.40
Cradle above bath level	1.97	939.32	0.59
Cradle opposite to bath	9.26	1408.30	2.79
Cradle opposite to metal	3.64	1622.32	1.09
Cradle opposite to block	17.25	390.02	5.19
Cradle opposite to brick	3.32	78.24	1.00
Cradle below floor level	36.38	99.59	10.95
Bar in to bar out	80.78		24.32
Cathode bottom estimate	196.81		59.26
-----			
Total Cathode Heat Lost	332.08		100.00

Table VI summarized the new 475 kA, 0.76 A/cm<sup>2</sup>, 2.8 cm ACD, 10.44 kWh/kg cell design results and compare them with the previous 520 kA cell design results.

Table VI: Design and predicted operational data

Amperage	520 kA	475 kA
Nb. of anodes	64	64
Anode size	1.95 m X .5 m	1.95 m X .5 m
Nb. of anode stubs	4 per anode	4 per anode
Anode stub diameter	17.5 cm	20.0 cm
Anode cover thickness	20 cm	20 cm
Nb. of cathode blocks	24	24
Cathode block length	4.17 m	4.17 m
Type of cathode block	HC10	HC10
Collector bar size	20 cm X 20 cm	20 cm X 20 cm
Type of side block	HC3	HC3
Side block thickness	7 cm	7 cm
ASD	30 cm	30 cm
Calcium silicate thickness	6.0 cm	6.0 cm
Inside potshell size	17.8 mX4.85 m	17.8 mX4.85 m
ACD	2.8 cm	2.8 cm
Excess AlF <sub>3</sub>	12.00%	12.00%
Anode internal drop (A)	210 mV	208 mV
Cathode internal drop (A)	124 mV	158 mV
External drop (A)	127 mV	90 mV
Anode panel heat loss (A)	286 kW	238 kW
Cathode total heat loss (A)	381 kW	332 kW
Operating temperature (D/M)	957.7 °C	958.1 °C
Liquidus superheat (D/M)	4.7 °C	5.1 °C
Bath ledge thickness (D/M)	22.8 cm	20.6 cm
Metal ledge thickness (D/M)	18.1 cm	15.9 cm
Current efficiency (D/M)	96.5%	96.2%
Internal heat (D/M)	679 kW	576 kW
Energy consumption	10.85 kWh/kg	10.44 kWh/kg

### Future work

As the results presented in Table VI indicate, the reduction of the ohmic resistance of the cell has reached its limit, the reduction of the cell voltage could only be achieved by further decreasing the anode current density.

In order to reach 10 kWh/kg, further reduction of the anode current density will be required, below 0.7 A/cm<sup>2</sup> most probably. At that very low current anode current density, is it possible to operate the cell below 5.0°C of cell superheat? If so, part of the remaining reduction of the cell heat loss will come from a further reduction of the cell superheat but not much should be expected to come for that. Not much extra should be expected to come from the reduction of the stub and collector bar heat loss either, as in

the present paper dimensions of the different elements have been pushed to their limits.

The author is hoping that the next opportunity will come from the design of new cathode lining insulating material that would remain good insulating material under cell operating conditions at high temperature for the entire life of the cell. The reduction of the anode panel heat loss through the increase of the gas temperature under the cell hood is the only alternative path short of recycling the cell heat loss.

### Conclusions

It turned out it is possible to reduce enough the heat dissipation of a cell to be able to operate that cell in thermal balance at the very low energy consumption level of 10.44 kWh/kg Al. Electrically, at 0.76 A/cm<sup>2</sup> of anode current density, this requires operating at the lowest achievable ACD, which is around 2.8 cm. It also requires a total ohmic resistance of the anode cathode and busbar corresponding to a total voltage drop of about 450 mV.

Thermally, this requires operating at close to if not the lowest possible cell superheat of around 5.0°C, a very high anode cover thickness, very high pier height, and using the “special” but not “new” design feature presented in this work to reduce the stubs and collector bars heat loss.

Electrically, it is easy to continue to decrease the cell internal heat production by decreasing the anode current density below 0.7 A/cm<sup>2</sup>. Clearly the challenge of designing a cell operating at 10.0 kWh/kg lies in achieving a cell design having the proper thermal insulation to dissipate so little heat or by recycling part of the cell heat loss.

### References

- [1] M. Dupuis, “Low Energy Consumption Cell Designs Involving Copper Inserts and an Innovative Busbar Network Layout”, *TMS Light Metals*, 2017, 693-703.
- [2] G. Bearne, D. Gadd and S. Lix, “The Impact of Slots on Reduction Cell Individual Anode Current Variation”, *TMS Light Metals*, 2007, 305-310.
- [3] A. Al Zarouni and al., “Energy and Mass Balance in DX+ cells during Amperage Increase”, *31<sup>st</sup> International Conference of ICSOBA, 19th Conference, Aluminium Siberia, Krasnoyarsk, Russia*, September 4 – 6, 2013, 494-498.
- [4] W. Haupin, “Interpreting the Components of Cell Voltage”, *TMS Light Metals*, 1998, 531-537.
- [5] P. Entner, HHCellVolt AIWeb application: <http://peter-entner.com/ug/windows/hhcellvolt/toc.aspx>
- [6] B. Welch, “Specific Energy Consumption and Energy Balance of Aluminium Reduction Cell”, *8th international congress "Non-ferrous metals & minerals", Krasnoyarsk, Russia*, September 13 – 16, 2016.
- [7] P. Entner and M. Dupuis, “Extended Energy Balance for Hall-Héroult Electrolysis Cells”, *12<sup>th</sup> Australasian Aluminium Smelting Technology Smelter*, 2018, to be published.
- [8] M. Dupuis, “Very Low Energy Consumption Cell Design: The Cell Heat Balance Challenge”, *TMS Light Metals*, 2018, 689-697.
- [9] M. Dupuis, “Breaking the 11 kWh/kg Al barrier”, *ALUMINIUM 94(1/2)*, 2018, 30-34.
- [10] M. Dupuis, “Using ANSYS to Model Aluminum Reduction Cell since 1984 and Beyond”, *Proceedings of the ANSYS 10th International Conference*, 2002, available only on CD.
- [11] J. N. Bruggeman, “Pot Heat Balance Fundamentals”, *Proc. 6<sup>th</sup> Aust. Al Smelting Workshop*, 1998, 167-189.
- [12] M. Dupuis and V. Bojarevics, “Retrofit of a 500 kA Cell Design into a 600 kA Cell Design”, *ALUMINIUM 87(1/2)*, 2011, 52-55.
- [13] B. Langon, “Carbonaceous Anode with Partially Constricted Round Bars Intended for Cells for the Production of Aluminium by Electrolysis”, *US Patent US4612105A*, 1986.
- [14] S. Becasse and al., “APXe Cell Technology 7 Years of Low Energy Operation”, *TMS Light Metals*, 2018, 699-704.
- [15] L. Mishra and al., “Anode Yoke, Anode Hanger and Anode Assembly for a Hall-Héroult Cell”, *Patent Application Number 1721141.8*, 2017.